Chapter 8
Co(II) complexes of fused heterocyclic ring systems

8.1. Introduction

The exploration of privileged structures in drug discovery has gained significant popularity in medicinal chemistry over the past years. Heterocycles play an important role in the design and discovery of new pharmacologically active compounds. Recently quinoxalines and related heterocycles were introduced as prospective potential chemotherapeutic drug candidates possessing manifold biological activities. Besides a wide spectrum of pharmacological activities, quinoxaline derivatives have been reported to possess anti-microbial and anti-inflammatory activities. Moreover fusion of tetrazole, which is considered as planar acidic heterocyclic analogue of carboxylic function, has the ability to increase potency and improve bioavailability[1-3]. Similarly Schiff bases apart from other biological activities have been reported to exhibit antimicrobial effect. In light of the above findings coupled with our interests in the chemistry of bridge head nitrogen heterocyclic systems gave us the idea for the synthesis of novel condensed heterocyclic compounds encompassing bioactive molecules, tetrazoles and quinoxalines with the aim to explore their potent biological activity for the first time. Lately, new biological effects as well as a number of biological targets for these compounds have been discovered, paving the way for drug like substances design on their basis.

8.2. Synthesis of ligands:

8.2.1. Synthesis of ligand 1 (L^1):

8.2.1.1. Synthesis of 3-chloro -2 hydrazinoquinoxaline (I) :

2, 3-dichloroquinoxaline (2.98g, 0.015mol) and hydrazine hydrate (1g, 0.02mol) in 50 ml of ethanol were refluxed for 3 h. The product obtained was filtered and recrystallised from rectified spirit. Yield (84%), m.pt. 187-190^{o}C, mass (m/z): 194.

8.2.1.2. Synthesis of 2-hydrazino tetrazolo-[1, 5-*a*]-quinoxaline (II) :

3-chloro-2-hydrazinoquinoxaline (3.89gm, 0.02mol) and sodium azide (1.30 g, 0.02mol) were refluxed for 2 h in an oil bath and with routine labor work-up yielded 2-hydrazinotetrazolo-[1,5-*a*]-quinoxaline (II). Yield 83%, m.pt: 187-189^{o}C, mass (m/z): 199.

8.2.1.3. Synthesis of 1-substituted benzylidenehydrazino-2(tetrazolo-[1, 5-a]

quinoxa lin-4-yl derivatives (III)

The compound **II** (2.01 g, 0.01mol) and salicylaldehyde (0.010mol) on refluxing with DMF afforded the solid product in good yield. It was recrystallised with methanol and dried. m.pt: 192-194^{o}C. IR(KBr) cm^{-1}: 3042 (Ar-CH), 3298 (-NH), 1587 (-N=N-), 1562 (>C=N), 1532 (>C-N). ^{1}H-NMR (DMSO-d^{6}): δ 6.96 – 7.95 (m, 8H, Ar-H), 3.87 (s, 1H, NH), 8.02 (s, 1H, -CH=N). Anal calcd (%) for $C_{15}H_{11}N_7O$ % C, 59.71; H, 3.35; N, 32.80; Found (%) : C, 59.74; H, 3.38; N, 32.83.

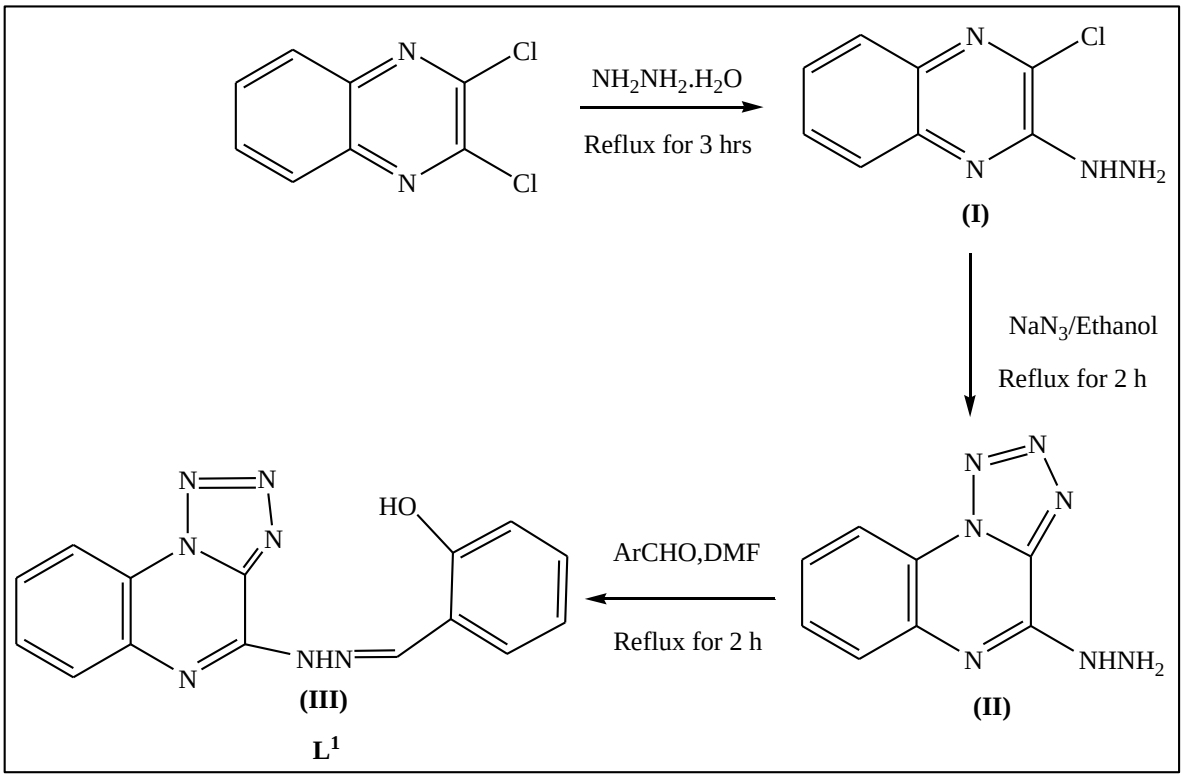

Scheme 1: Synthesis of ligand 1 (L^1)

8.2.2. Synthesis of ligand 2 (L^2):

2,3-dichloroquinoxaline (0.19g, 0.001mol) and 4-amino-5-pyridin-4-yl-*4H*-[1,2,4]triazole-3-thiol (0.19g, 0.001mol) in 50 ml of DMF were refluxed for 3 h. The product obtained was filtered and recrystallised from dichloromethane. Yield (84%), m.pt. 192-194^{o}C, mass (m/z): 319.13. IR (KBr) cm^{-1}: 3042 (Ar-CH), 3318 (-NH), 1656 (C=N), 1533 (C-N). ^{1}H-NMR (DMSO-d^{6}): δ 7.35 – 8.04 (m, 8H, Ar-H), 5.03 (s, 1H, NH). Anal calcd (%) for $C_{15}H_{19}N_7S$ % C, 56.42; H, 2.84; N, 30.70; Found (%) : C, 56.34; H, 2.88; N, 30.74.

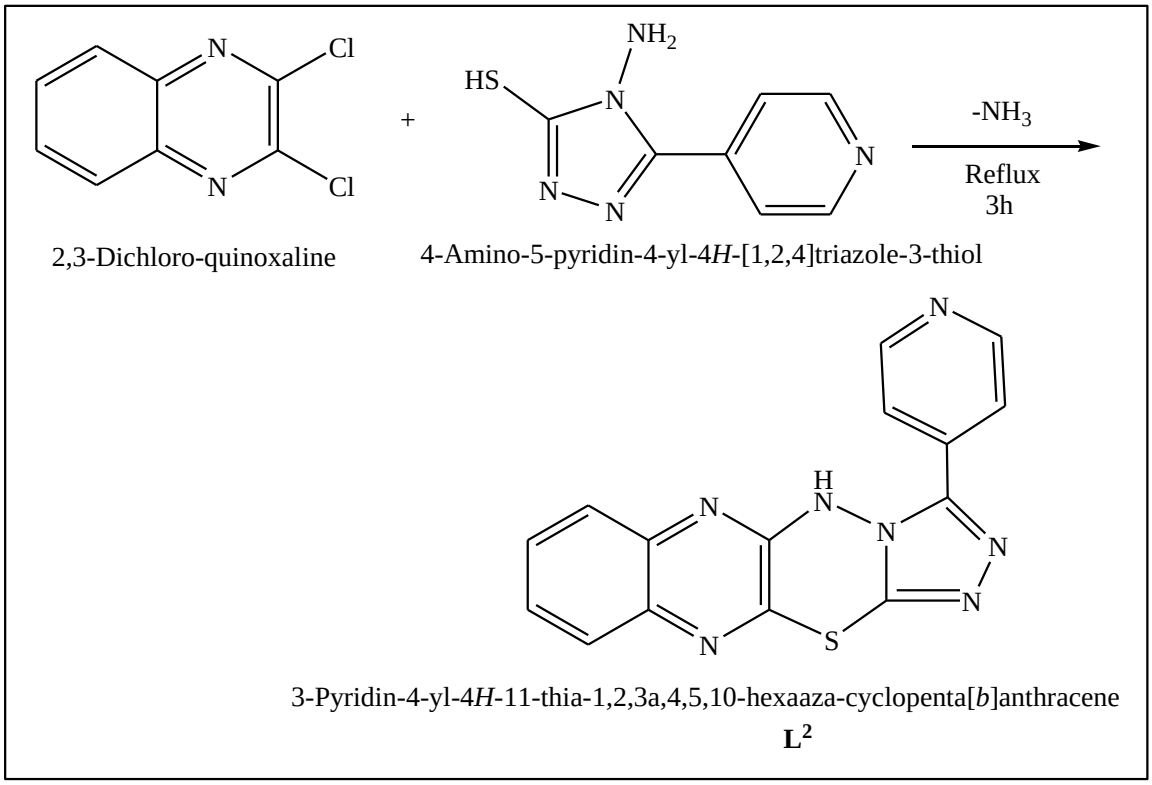

Scheme 2: Synthesis of ligand 2 (L^2)

8.2.3. Synthesis of ligand 3 (L^3)

2,3-dichloroquinoxaline (0.19g, 0.001mol) and 4-amino-5-pyridin-4-yl-*4H*-[1,2,4]triazole-3-thiol (0.19g, 0.001mol) in 50 ml of DMF were refluxed for 3 h. The product obtained was filtered and recrystallised from dichloromethane. Yield (84%), m.pt. 192-194^{o}C, mass (m/z): 319.13. IR (KBr) cm^{-1}: 3042 (Ar-CH), 3318 (-NH), 1656 (C=N), 1533 (C-N). ^{1}H-NMR (DMSO-d^{6}): δ 7.35 – 8.04 (m, 8H, Ar-H), 5.03 (s, 1H, NH). Anal calcd (%) for $C_{15}H_{19}N_7S$ % C, 56.42; H, 2.84; N, 30.70; Found (%) : C, 56.34; H, 2.88; N, 30.74.

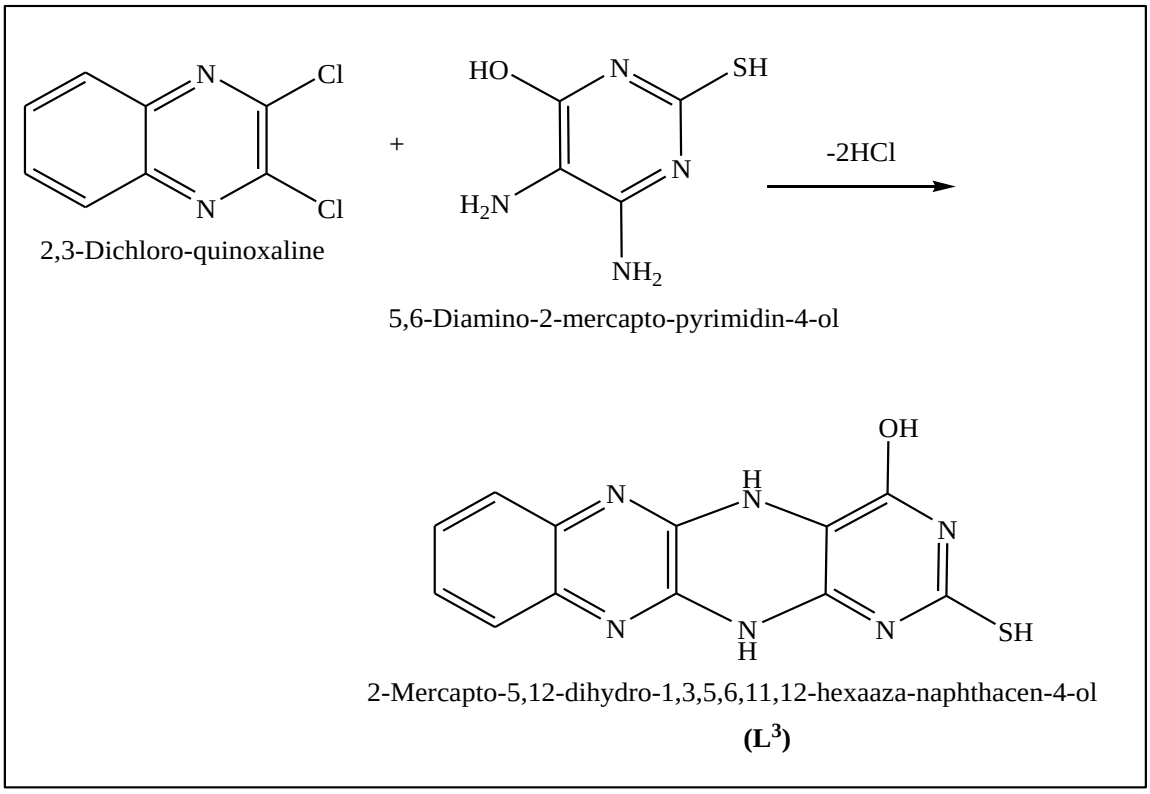

Scheme 3: Synthesis of ligand 3 (L^3)

8.3. Synthesis of complexes

8.3.1. Synthesis of Co(II) complex 4 :

A methanolic solution (20 mL) containing **L^1** (0.334 g, 1mmol) and cobaltous chloride (0. 2g, 1mmol) were added and refluxed for 5h. The resulting mixture was then cooled to room temperature, which resulted in the formation of orange colour precipitate. It was filtered off and the solid was recrystallised from ethanol .Yield: 65%. m.pt: 241-244°C. Anal. calcd (%) for $C_{16}H_{15}ClCoN_7O_2$: C, 44.51; H, 3.50; N, 22.71,Found(%):C,44.17;H,3.56;N,22.45.

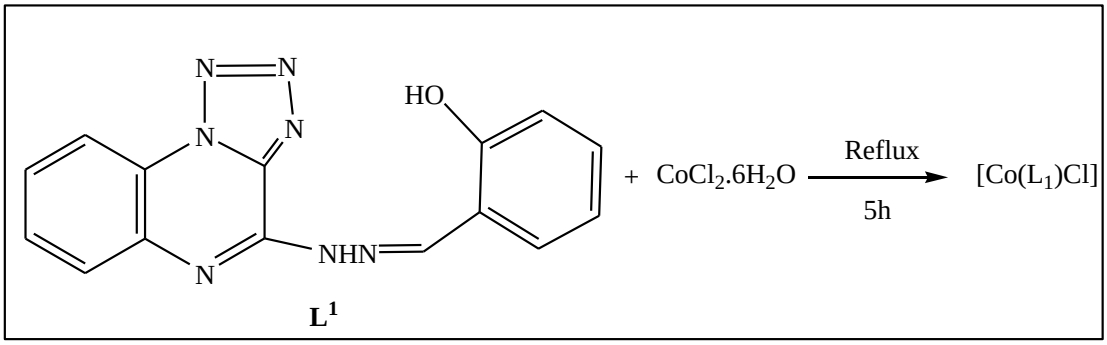

Scheme 4 : Synthesis of Co(II) complex 4

8.3.2. Synthesis of Co(II) complex 5 :

A methanolic solution (20 mL) containing **L^2** (0.319 g, 1mmol) and cobaltous chloride (0. 2g, 1mmol) were added and refluxed for 5h. The resulting mixture was then cooled to room temperature, which resulted in the formation of dark brown coloured precipitate. It was filtered off and the solid was recrystallised from ethanol .Yield: 65%. m.pt: 241-244°C. Anal. calcd (%) for $C_{30}H_{22}Cl_2CoN_{14}S_2$: C, 46.61; H, 2.87; N, 25.38, Found (%): C, 46.57;H,2.76; N,25.51.

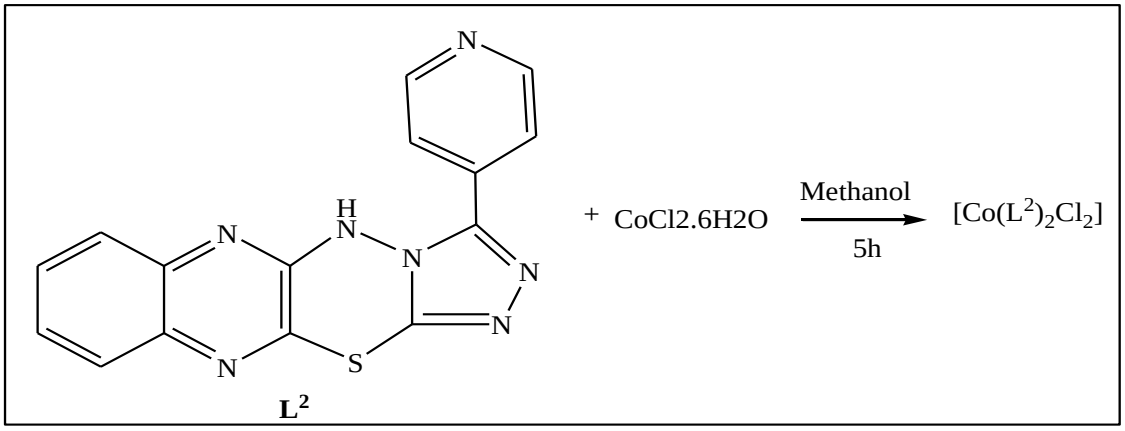

L^2

Scheme 5 : Synthesis of Co(II) complex 5

8.3.2. Synthesis of Co(II) complex 6:

A methanolic solution (20 mL) containing **L^3** (0.288 g, 1mmol) and cobaltous chloride (0. 2g, 1mmol) were added and refluxed for 5h. The resulting mixture was then cooled to room temperature, which resulted in the formation of brown coloured precipitate. It was filtered off and the solid was recrystallised from ethanol .Yield: 65%. m.pt: 241-244°C. Anal. calcd (%) for $C_{30}H_{22}Cl_2CoN_{14}S_2$: C, 46.61; H, 2.87; N, 25.38, Found (%): C, 46.57;H,2.76; N,25.51.

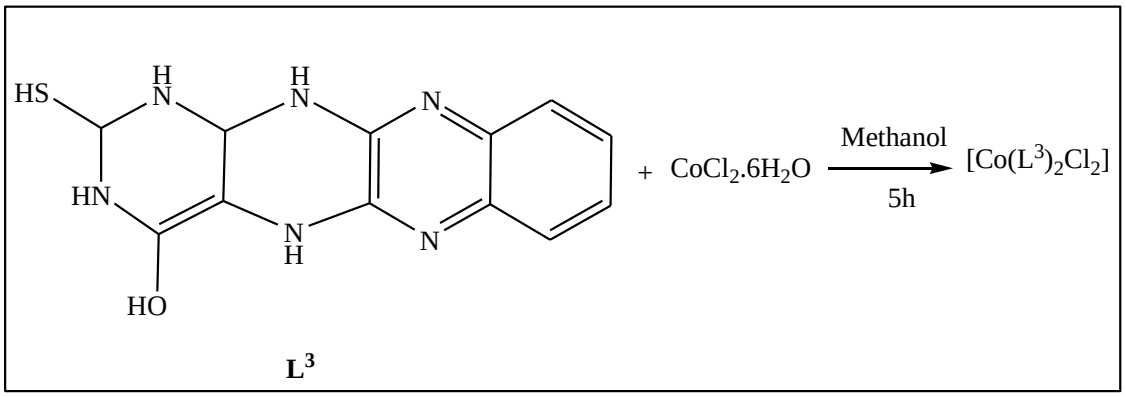

L^3

Scheme 6: Synthesis of Co(II) complex 6

8.4. Results and discussion

8.4.1. Structural description of the ligands

The synthesized ligand is characterized using various spectral techniques like FT-IR, electronic spectra and ^{1}H-NMR. In the ^{1}H-NMR spectra, the integral intensities of each signal were found to agree with the number of different types of protons present in the complex. A signal appeared in the ^{1}H-NMR spectrum of the ligand **L^{1}** at δ 8. 02 ppm is characteristic of >CH=N proton. The signals appeared at δ 3.80 and δ 4.60 ppm is attributed to the >NH and the -OH protons respectively. The aromatic protons are observed in the region δ 6.96– 7.95 ppm.

The ^{1}H-NMR spectrum of the ligand **L^{2}** shows the following signals at the following ppm values; δ 7.35 – 8.04 ppm due to the aromatic protons and δ 5.03ppm due to the >NH protons. The ^{1}H-NMR spectrum of the ligand **L^{3}** shows the following signals at the following ppm values; δ 6.90 ppm and δ 7.10 ppm due to the aromatic protons, δ 4.40 ppm due to SH proton, δ 3.60 ppm due to NH proton and δ 13.80 ppm due to hydroxyl proton. These values confirm the structure of the ligands and their NMR spectrum are shown in Figs. 8.1a to 8.1c for L^{1}, L^{2} and L^{3} respectively.

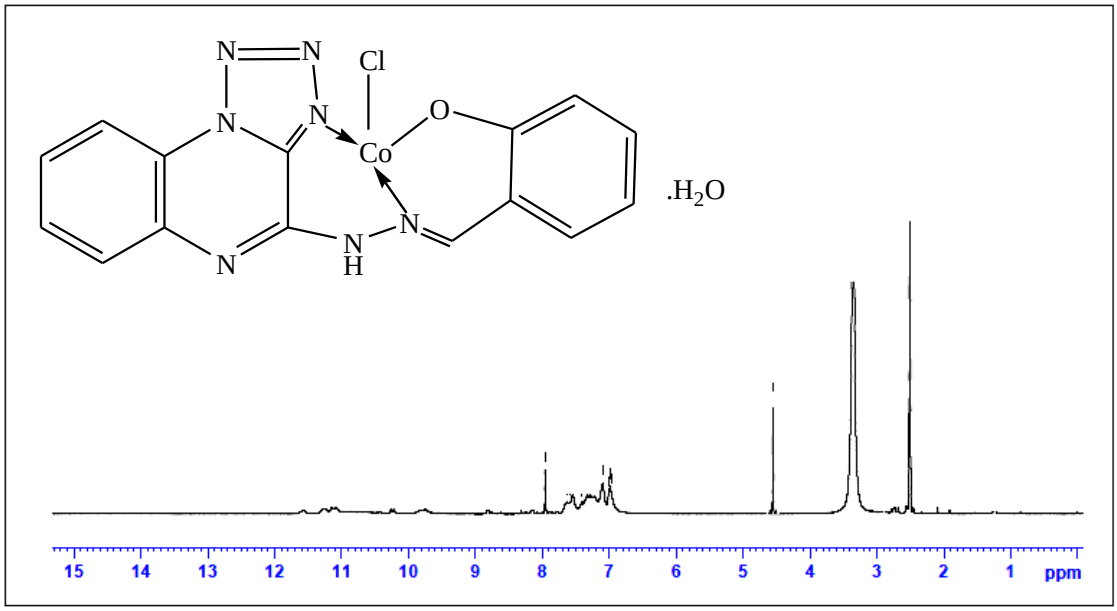

Fig.8.1a. ^{1}H-NMR Spectrum of Ligand 1 (L^{1})

8.4.2. FT-IR spectra

The prominent infrared spectral data of the ligand and its metal complexes are presented in Table 8.1. The FT-IR spectrum of the ligand ($\mathbf{L^1}$) shows band at 3398 cm^{-1} which can be attributed to phenolic –OH group. This band also appeared in the complex **4** creating a doubt about the co-ordination of phenolic –OH with the metal but the involvement of deprotonated phenolic –OH group in Co(II) complex **4** is confirmed by the shift of γ(C-O) stretching band observed at 1203 cm^{-1} in the free ligand to higher frequency at 1221 cm^{-1} proving its co-ordination. The azomethine and C=N(thiazole) vibration of the ligand at 1562 cm^{-1} and 1434 cm^{-1} was shifted to lower frequency after complexation respectively confirming the co-ordination to the metal. The unchanged band after complexation at 1587cm^{-1} in the free ligands suggesting the non-involvement of N=N.

The FT-IR spectral values of ligand **2** ($\mathbf{L^2}$) and its complex **5** are as follows; the –NH stretching frequency of the ligand and the complex appears around 3300cm^{-1}. The >C=N stretching frequency of the quinoxaline ring in the ligand appeared at 1680cm^{-1} and this has been shifted to 1656cm^{-1} proving its co-ordination to the metal. The other stretching frequencies like >N-N< , >C=N (thiazole) appears at 1442, 1527 cm^{-1} in the ligand and its Co(II) complex proving its non-involvement in co-ordination.

The FT-IR spectral values of ligand **($\mathbf{L^3}$)** and its complex **6** are as follows; the –NH and the –OH stretching frequencies appears around 3300cm^{-1}. The >C=N stretching frequency in the ligand appears at 1674 cm^{-1} and this has been shifted to 1615 cm^{-1} proving its co-ordination to the metal. The other stretching frequencies like >C=N (pyrimidine), C=S, appears at 1530 and 1393 cm^{-1} for the ligand and 1528 and 1390 cm^{-1} in the complex and the appearance of these bands at same region without considerable shift in the complexes show the non-involvement of these groups in co-ordination[4-6]. The stretching frequencies of the ligand and the complexes are shown in Table 8.1 and the FT-IR spectra of the ligand and the complexes **(1-6)** are shown in Fig. 8.2a to 8.2f respectively.

Table 8.1. IR stretching frequencies of the ligand and the Co(II) complexes in cm^{-1}

Ligand 1 amd its Co(II) complex			
	C=N (imine)	**C=N(thiazole)**	**N=N**
L^1	1562	1434	1587
$[Co(L^1)Cl]$	1530	1421	1590
Ligand 2 and its Co(II) complex			
	C=N	**N-N**	**C=N(thiazole)**
L^2	1680	1442	1527
$[Co(L_2)_2Cl_2]$	1656	1442	1527
Ligand 3 and its Co(II) complex			
	C=N(pyrimidine)	**C=N(quinoxaline)**	**C=S**
L^3	1530	1674	1393
$[Co(L_3)_2Cl_2]$	1528	1615	1390

8.4.3. Electronic spectra

The electronic spectra of the ligand and the complexes were recorded using DMSO as the solvent. The cobalt(II) complex exhibited four bands having λ_{max} at 298, 368, 432 and 440 nm (Fig. 8.3).

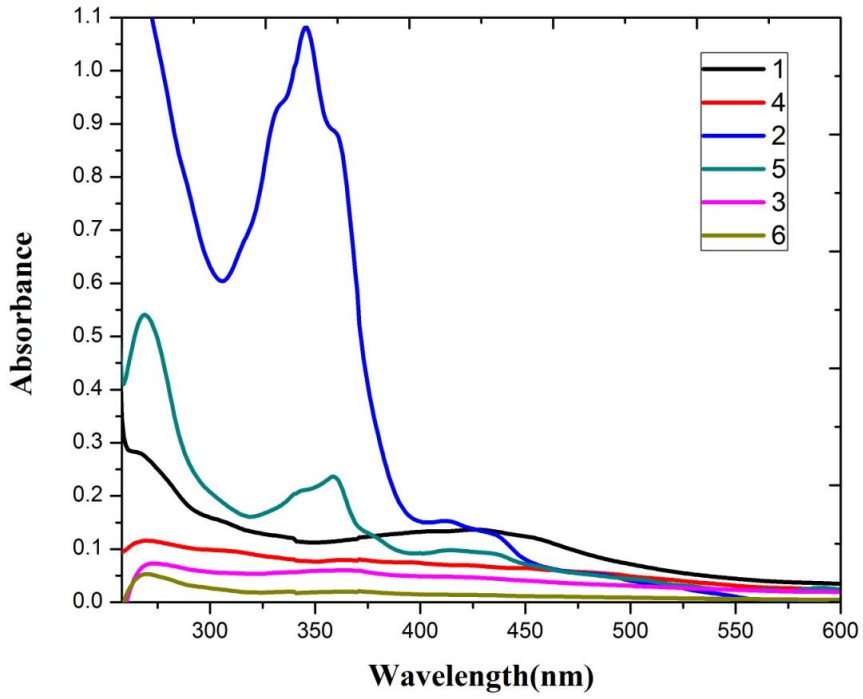

Fig. 8.3. Electronic spectrum of the complexes

The band at 328 nms assigned to charge transfer band and last three bands could be assigned for corresponding d-d transitions, due to

$^4T_{1g} \rightarrow {}^4T_{2g}$, $^4T_{1g} \rightarrow {}^4A_{2g}$ and $^4T_{1g} \rightarrow {}^4T_{1g}$ which justified the octahedral geometry of Co(II) complex. The analytical, CHN analysis and metal estimation data, it seems to be tetrahedral complex and the characteristic band at 611 nm is absent due to the involvement of DMSO in the trans position making it distorted octahedral geometry in solution state[7,8].

8.4.4.Thermal analysis

The simultaneous TGA/DTA analysis of the Co(II) complexes of the three ligands was studied from ambient temperature to 1000 °C under nitrogen atmosphere[9]. The TGA curve of the Co(II) complex **4** exhibited a mass loss at 51.42°C which corresponds to the loss of lattice water, and the chloride and the organic part of the complex is lost at two different stages at 325.66 °C and 466.02 °C with a total mass loss of 82.11 % (calcd.81.90 %) and leaving 17.89% CoO as residue (calcd. 16.95%).

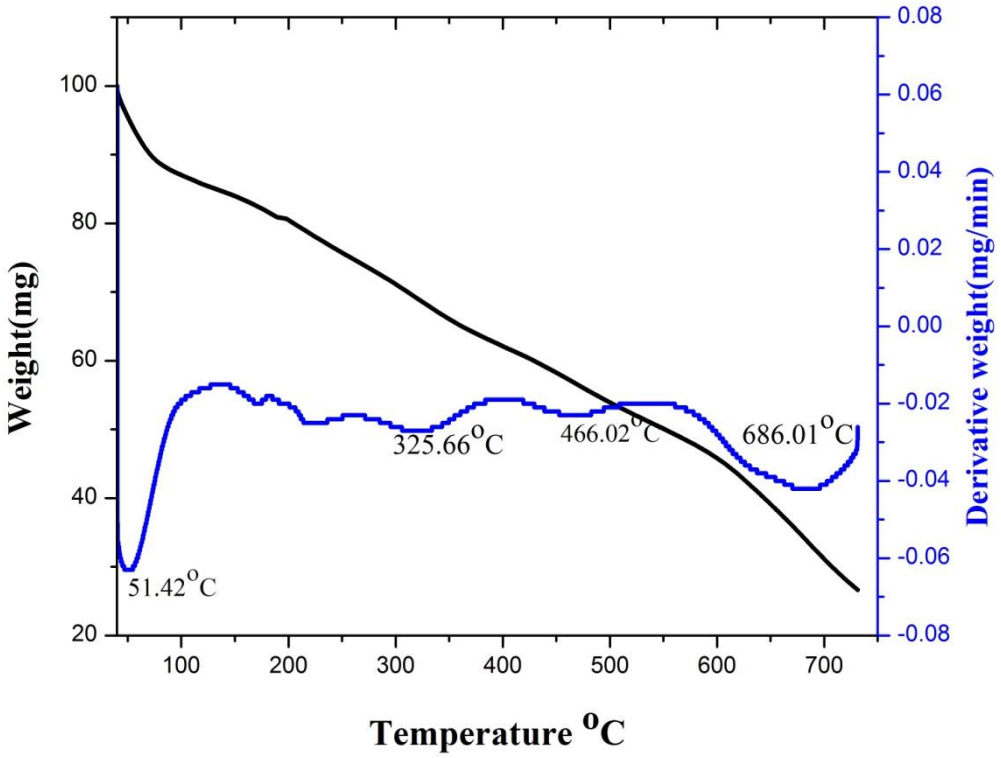

Fig. 8.4a. Thermogram of Co(II) complex 4

The TGA/DTA curve of the Co(II) complex **5** exhibited a mass loss at 253.60 °C and 380.29 °C which is attributed to the co-ordinated part of the ligand and chloride molecule. The stability of the complex till 253.60°C shows the absence of lattice and co-ordinated water molecule. The total mass loss is 86.77 % (calcd. 85.12 %) with CoO as residue. The TGA curve of the Co(II) complex **6** shows a single decomposition peak at 286.37 °C for the loss of organic fragments leaving behind CoO as residue with 18.76 % (calcd. 12. 34 %). The thermograms of the complexes are given in Figs. 8.4a to 8.4c respectively. The proposed geometry of the complexes is given in Fig. 8.5.

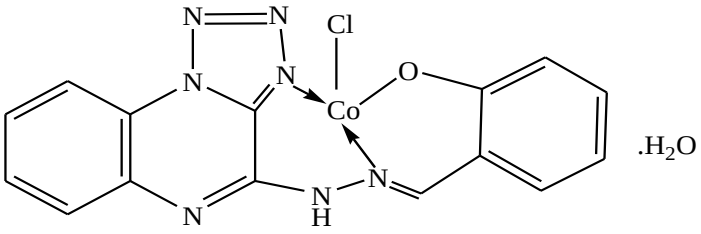

4

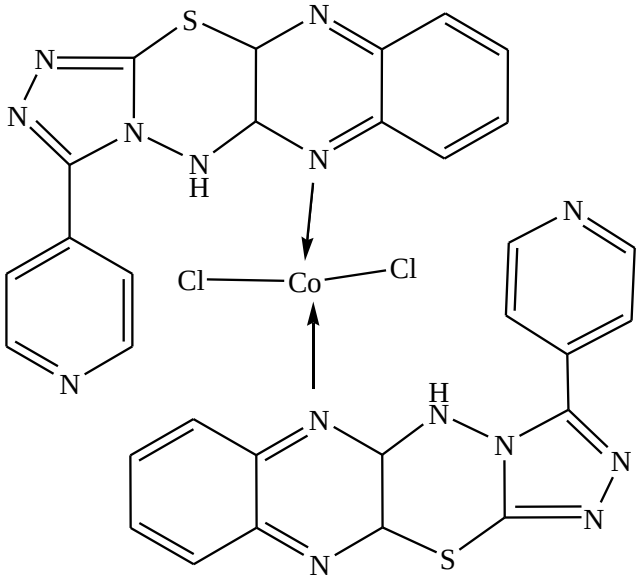

5

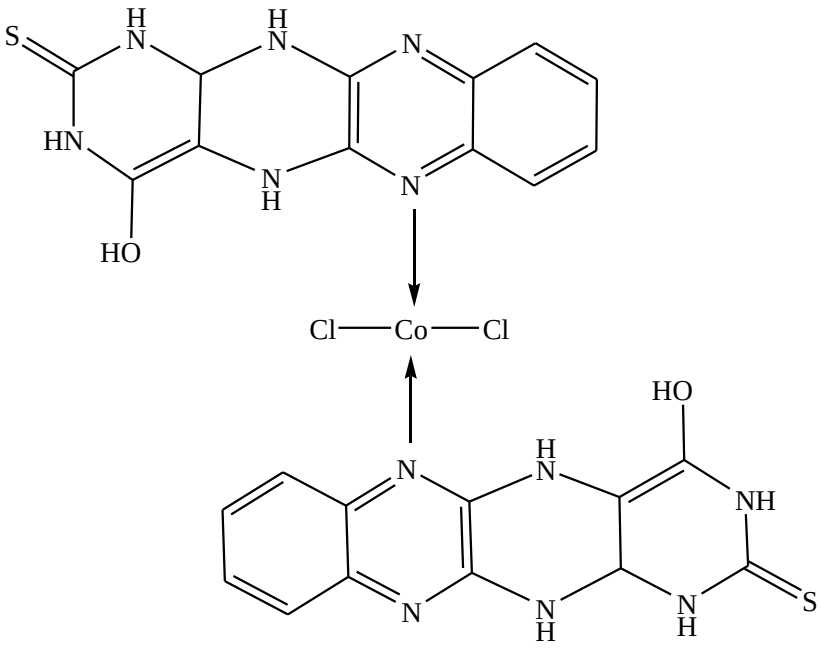

6

Fig. 8.4c. Proposed geometry of the complexes

8.4.5. Photoluminescence spectra

The photoluminescence properties of the Schiff base ligand and their complexes were studied at room temperature for 10^{-4} M solution for all compounds in DMSO solution. Excitation and emission slit widths were set at 10 nm with a scan speed of 500 nm/min. The emission spectra shows a maximum at 450 nm. The Co(II) complex of ligand **2** show the strongest quenching compared to ligand **1** and its complex. The photoluminescence intensities of the metal complexes changed with respect to that of the ligand upon complexation. As shown in Fig. 8.6a, the ligand exhibited an emission at 410nm which shifted to 445nm upon binding to the cobalt metal ion. A decrease in the emission intensity was observed depending on complex formation with cobalt metal ions with ligand **1** and **2**, and an increase in the emission intensity with ligand **3**. Thus it is evident that the fluorescence emission intensity of the ligand decreases dramatically depending on the complex formation with the Co(II) metal ions. The decrease of emission intensities is due to the formation of the co-ordination complex with N atoms[10].

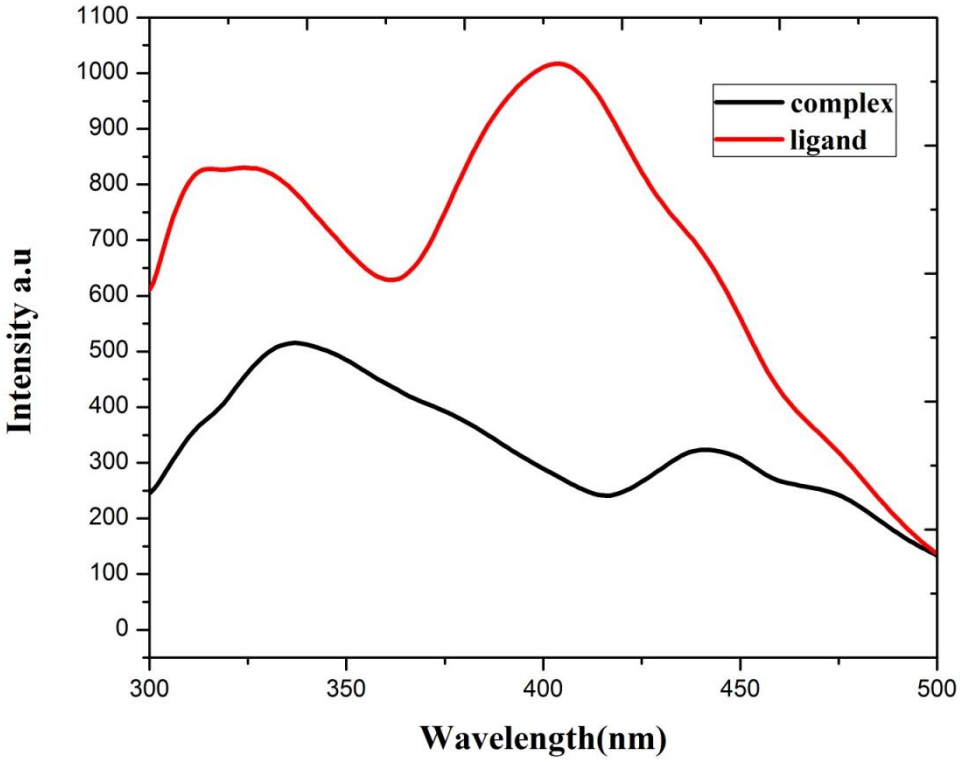

Fig. 8.6a. Fluorescence spectra of the ligand L^1 and its Co(II) complex 4

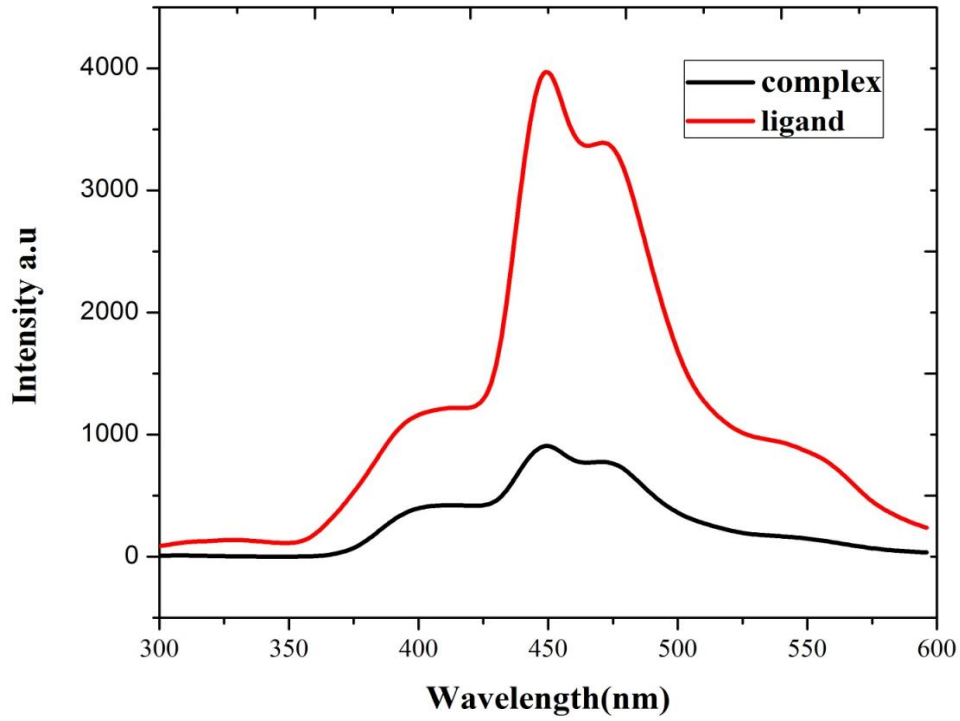

Fig. 8.6b. Fluorescence spectra of the ligand L^1 and its Co(II) complex 5

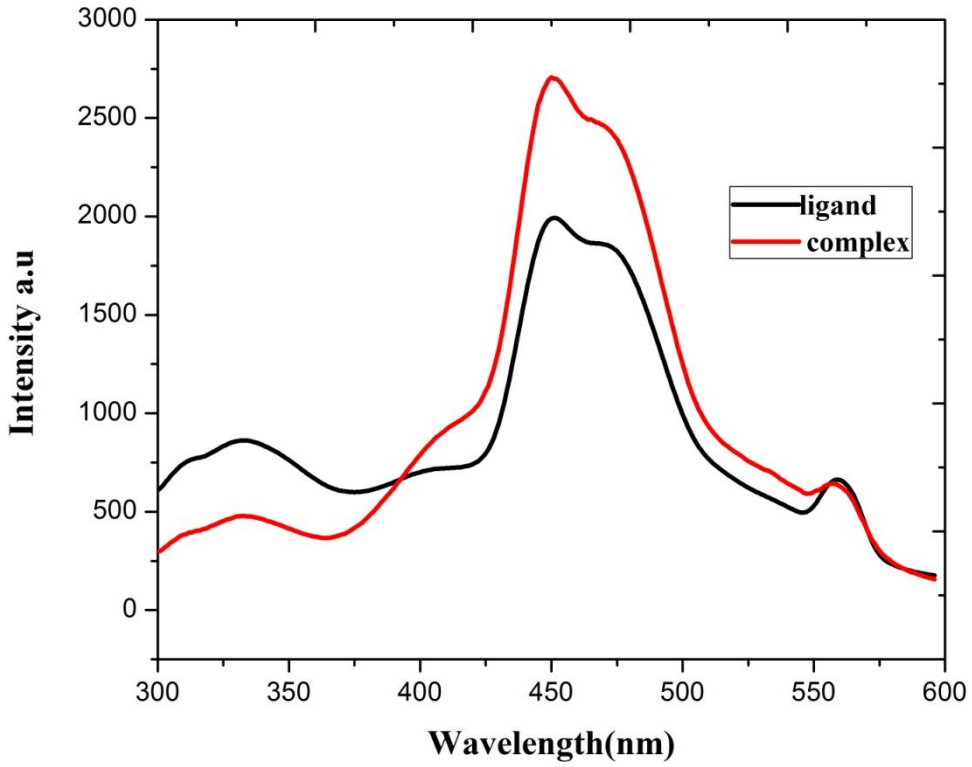

Fig. 8.6c. Fluorescence spectra of the ligand L^1 and its Co(II) complex 6

These coordination complexes make the energy transfer possible from the excited state of the ligand to the metal ions, thus increasing the nonradiated transition of the ligand excited state and decreasing the fluorescence emission. This clearly implicates an interaction between the metal ion and the ligand. Quenching of fluorescence of the ligand by transition metal ions during complexation is a rather common phenomenon, which can be explained by processes including magnetic perturbation, redox-activity, and electronic energy transfer. Enhancement of fluorescence through complexation is, however, of much interest, as it opens up the opportunity for photochemical applications of these complexes. It can be seen in Fig. 8.6c that upon complexation of the ligand, the photoluminescence intensities of the metal complexes increase. The increase in intensity is due to the formation of a metal-to-ligand ratio of 1:2, resulting in larger molecule formation. There are 2 driving forces competing here: the interaction between the metal and ligand due to complexation results in a reduction of photoluminescence intensities, while the formation of the metal-to-ligand ratio of 1:2 leads to an increase in photoluminescence intensities and thus the formation of larger molecules. Additionally, upon complexation of the ligand, the maximum photoluminescence peak shifted from 410 to 445 nm, other peaks and shoulder peaks became more intense and obvious. Some electrons of the atoms or moieties of this

ligand become affected by the inserted metal ions. This emission wavelength difference can probably be used for tuning in photoluminescent devices. The photoluminescent properties of these compounds may indicate a great deal of potential for numerous optical and electronic applications.

8.5. Pharmacology

8.5.1. Anti-microbial activity

The ligands and the Co(II) complexes were prepared and tested for their *in vitro* antimicrobial activity against six strains of microbes, which are *Escherichia coli, Pseudomonas aeruginosa, Staphylococcus aureus, Klebsiella pneumoniae, Aspergillus niger* and *Candida albicans*. It was observed that the synthesized compounds showed very good antimicrobial properties. The compounds $[Co(L_2)_2Cl_2]$ and $[Co(L_3)_2Cl_2]$ were excellently equipotent against the microbial strain , *S. aureus***,** and moderately active against other test organisms**.** $[Co(L_2)_2Cl_2]$ and $[Co(L_3)_2Cl_2]$ showed optimum equipotent activity against *P.aeroginosa* and *K.pneumonia*. $[Co(L_3)_2Cl_2]$ show pronounced activity against *A. niger* and significant activity against *C. albicans.* $[Co(L^1)Cl]$ is mild active against the strains and the ligand is less active when compared to that of the complexes.

Table 8.2. *In-vitro* antimicrobial screening data of the ligand and its Co(II) complexes (MIC in µg/ml)

Compound	*E.coli*	*P.aeroginosa*	*S.aureus*	*K.pneumonia*	*A.niger*	*C.albicans*
L^1	>500	125	125	250	250	>500
L^2	>500	62.5	62.5	125	125	>500
L^3	>500	62.5	62.5	125	125	>500
$[Co(L^1)Cl]$	250	16.12	8.00	16.12	31.25	125
$[Co(L_2)_2Cl_2]$	125	8.00	4.00	8.00	31.25	62.5
$[Co(L_3)_2Cl_2]$	62.5	8.00	4.00	8.00	16.12	31.25
Ofloxacin	2.00	2.00	2.00	2.00	-	-
Griseofulvin	-	-	-	-	8.00	8.00

Thus the presence of more heteroatoms and metal ion seems to be of great significance for antimicrobial efficacy[11,12].

8.5.2. DNA Cleavage activity

The synthesized Co(III) complexes has been subjected to nuclease activity in the presence of radical scavengers. There are two possible mechanisms

known to play a role in the cleavage by metallonucleases: hydrolytic and oxidative. The hydrolytic mechanism of cleavage relies on the inductive effects of the metal on the phosphate backbone. This interaction increases the susceptibility of the phosphate backbone toward nucleophilic attack by bulk water or hydroxide thus produing the linearization of DNA observed as a result of complex cleavage. The oxidative mechanism of cleavage functions primarily through the production of reactive oxygen species and can include hydroxyl radical and singlet oxygen species that are produced via the Co(II)/Co(III) redox couple.

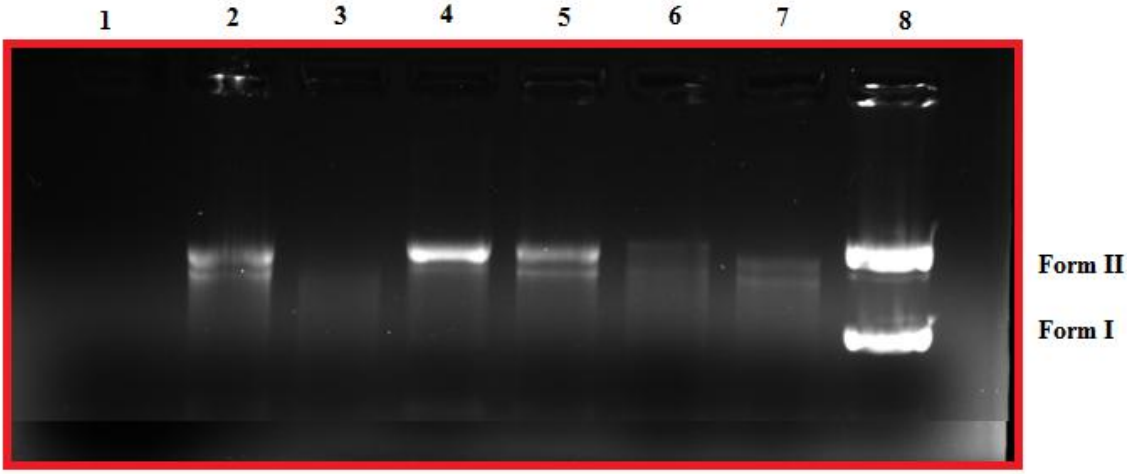

Fig.8.7. Changes in the agarose gel electrophoretic pattern of pBr322 DNA induced by H_2O_2 and Co(III) complexes , lane 1, DNA alone; lane 2, DNA + H_2O_2; lane 3, DNA(20μM) + 4 + H_2O_2; lane 4, DNA(40 μM) + 4 +H_2O_2; lane 5, DNA(20μM)+5+ H_2O_2; lane 6, DNA(40 μM) + 5 + H_2O_2; lane 7, DNA(20 μM) +6+H_2O_2, lane 8, DNA(40 μM) +6+H_2O_2.

To elucidate the mechanism of DNA strand scission by complexes **4-6** (hydrolytic or oxidative), cleavage reactions were carried out in the presence of hydrogen peroxide. The results are presented in Fig. 8.7. The lane **1** and **2** showing studies with DNA alone revealed no change in nuclease activity. From the lanes **3** to **8** the Co(III) complexes with two different concentrations 20μM and 40μM. There is no cleavage activity ie neither complex can completely convert super-coiled DNA (I) to single nicked (II) with concentrations upto 40 μM. For both complex **4** and **5,** there is no such cleavage at 10μM. At 20 μM, there is minimal amounts of form II formed for the complexes. The Co(III) complex **6,** at 10μM there is only very less amounts of form II

formed, but at 20 μM, the complexes show both form I and form II. Overall, these results suggest that complexes **4-6** utilize an oxidative mechanism to cleave DNA.

8.6. Conclusion

Co(II) complexes of fused heterocyclic compounds has been synthesized and characterized using various spectral techniques like FT-IR, electronic spectra, NMR, TGA techniques. From the results of the spectral data, a tetrahedral geometry has been suggested for the complexes. The emission properties of the ligand and the complexes has been studied and compared. In complexes **4** and **6**, quenching has taken place and in complex **5**, the intensity of the complex has increased. These results indicate the photoluminescent properties of these compounds and these find a great deal of potential for numerous optical and electronic applications. The in-vitro antimicrobial activity of the ligand and the complexes has been compared, the complexes are found to be more active than that of the ligand. The DNA cleavage activity of the complexes has been studied and found to follow non-oxidative mechanisms. These results prove that these complexes are biologically active and can be aimed for the future research for pharmaceutical applications.

References

1. Umarani N, Ilango K, Narendra Kumar S, *Der pharma chemica*, **2** (2010) 159.
2. Parvin K, Ashwani K, Jag Mohan L, Makrandi J K, *Bull. Korean Chem Soc*, **31** (2010) 3304.
3. Jagmohan L, Ashok K, *Indian J Chem*, **42B** (2003) 1463.
4. Gulcan M, Sonmez, Berber I, *Turk J Chem*, **36** (2012) 189.
5. Carmen R, Quiros M, Sala J M, *Polyhedron* **27** (2008) 2779.
6. Ana B, Salas J M, *Polyhedron* **33** (2012) 137.
7. Kalia S B, Lumba K, Kaushal G, Sharma M, *Indian J Chem*, **46A** (2007) 1233.
8. Raman N, Muthuraj, Ravicahndran S, Kulandaisamy A, Proc Indian Acad Sci(chem. Sci), **115** (2003) 161.
9. Munde A S, Jagdale A M, Jadhav S M, Choudhekar T K, *J Serb Chem Soc*, **75** (2010) 349.
10. Onal Z, Zengin H, Sonmez M, *Turk J Chem*, **35** (2011) 905.

11. Gurbez D, Cinarli A, Tavman A, Tau A, *Bull Chem Soc Ethiopia,* **29** (2015) 63.
12. Jone Kirubavathy S, Velmurugan R, Karvembu R, Bhuvanesh N S P, Parameswari K, Chitra S, *Russ J Co-ord Chem* **41** (2015) 345.
13. Ramsey A S, David F, Han X, Bruce K, Kristin M, Lynne C, Joseph M, Laurie A, *J Inorg Biochem*, **137** (2014) 1.